Electronic Supplementary Material (ESI) for Journal of Materials Chemistry A.

Electronic Supplementary Information

In situ growth of Ag_2S quantum dots on SnS_2 nanosheet with enhanced charge separation efficiency and CO_2 reduction performance

A. Putta Rangappa,[a] D. Praveen Kumar,[a] Jinming Wang,[a] Khai H. Do,[a] Eunhyo Kim,[a] D. Amaranatha Reddy,[b] Hyun S. Ahn,*[a] Tae Kyu Kim*[a]

[a] *Department of Chemistry, Yonsei University, Seoul 03722, Republic of Korea*

[b] *Department of Sciences, Indian Institute of Information Technology Design and Manufacturing, Kurnool 581007, Andhra Pradesh, India*

---

*Corresponding authors.

E-mail) tkkim@yonsei.ac.kr (T.K.K.) and ahnhs@yonsei.ac.kr (H.S.A.)

Synthesis of Ag_2S nanoparticles

To understand the basic band structure and photo-physical properties of pure Ag_2S, the Ag_2S nanoparticles were synthesized from the solutions of silver nitrate ($AgNO_3$, 50 mmol) and sodium sulfide pentahydrate ($Na_2S.5H_2O$, 25 mmol) in the presence of trisodium citrate dihydrate ($Na_3C_6H_5O_7.2H_2O$, 5 mmol) as stabilizing agent. Initially the silver nitrate solutions were prepared by dissolving them into 200 mL of water under vigorous stirring. The obtained solutions were added dropwise into the solution containing the trisodium citrate and sodium sulfide pentahydrate. After continued stirring in the dark for 24 hours, the resulted products collected by several washes with water and ethanol and then air dried at 80 °C overnight to obtain pure Ag_2S nanoparticles.

Characterizations

The photocatalysts were characterized by powder X-ray diffraction (XRD), X-ray photoelectron spectroscopy (XPS), transmission electron microscopy (TEM), diffuse reflectance spectrophotometry (DRS), and photoluminescence (PL) spectrometry techniques. XRD patterns were collected on a Bruker D8 Advance diffractometer using Cu K_α radiation. XPS measurements were performed using Al K_α radiation (1486.6 eV) with an energy of 15 kV/150 W. TEM and high-resolution-TEM (HRTEM) measurements were undertaken using a JEOL JEM-2100F operated at an acceleration voltage of 200 kV. DRS spectra were recorded on a Shimadzu UV-1800, and PL properties were studied on a Hitachi F-7000 fluorescence spectrometer. Time-resolved fluorescence spectra (TRFS) were measured on a femtosecond fluorescence spectrophotometer (Edinburgh FES 920). Raman spectra were obtained using a Horriba Jovin Yvon spectrometer equipped with an Nd:YAG laser (532 nm). EPR spectra were recorded on Bruker EMX/Plus spectrometer by using 3 mW power at room temperature and the modulation frequency, amplitudes were 100 kHz and 5 G respectively. The isotopic labelling experiments for $^{13}CO_2$ products were recorded by using $^{13}CO_2$ gas (isotope purity 99% and chemical purity 99.9 %, Tokyo Gas Chemicals Co. Ltd. of Japan) as the carbon source with the same photo experimental conditions and the products were analyzed by gas chromatography-mass spectrometry (JMS-K9, JEOL-GCQMS, Japan).

Photoelectrochemical measurements were carried out on a CHI 617B electrochemical analyzer and three-electrode system, with Pt wire and Ag/AgCl as the counter electrode and reference electrodes, respectively. The working electrode was prepared by spinning a photocatalyst suspension containing Nafion solution (30 μL, 0.02 mg μL^{-1}) onto In-doped SnO_2-coated glass, which was then placed in an oven at 100 °C for 3 h to dry the solvent and solidify the samples. Photocurrent curves were measured in Na_2SO_4 electrolyte (0.5 mol L^{-1}) during the on/off period of the 150-W Xe lamp solar simulator equipped with an AM 1.5G filter. Mott-Schottky experiments were conducted at a frequency of 1 kHz. The process was consistent, other than the dark condition.

Since different electron numbers are involved in producing the CO and CH_4, total consumed electron number (TCEN) was measured (Table S3) to assess the overall photocatalytic activity for CO_2 reduction in the system using the following equation:

$$\mathrm{TECN} = \frac{\left(2n_{\mathrm{CO}} + 8n_{\mathrm{CH_4}}\right)V_{REA}}{m_{CAT} + t_{IRR}} \quad (1),$$

where V_{REA} is the volume of the reactor, m_{CAT} the mass of the photocatalyst, t_{IRR} the light irradiation time and n_{CO} and $n_{\mathrm{CH_4}}$ is the produced CO and CH_4 amount in unit time, respectively. Apparent quantum yield (AQY) is defined as the ratio of number of reacted electrons to the number of incident photons and was calculated by following equation:

$$\mathrm{AQY}(\%) = \frac{\text{Number of reacted electrons}}{\text{Number of incident photons}} = \frac{\left(2n_{\mathrm{CO}} + 8n_{\mathrm{CH_4}}\right)N_A}{\text{Number of incident photons}} \times 100\ (\%) \qquad (2),$$

where N_A is the Avogadro's number. The number of incident photons is calculated based on the following equation:

$$\text{Number of incident photons} = \frac{\text{Absorbed photon by photocatalyst}}{\text{Averaged photon energy}} = \frac{H \times A}{\left(hc/\lambda\right)} \times t_{IRR} \qquad (3),$$

where H is the apparent light input at the photocatalyst (100 W m^{-2}) measured by using standard Si reference cell (Abet technologies), A the geometric irradiation area of the photocatalyst (3.88 cm^2), where h Planck's constant (6.626×10^{-34} J s), c the speed of light (3.0×10^{8} m s^{-1}). The wavelength of the light was estimated based on the estimated bandgap of SnS_2/Ag_2S-50, because the electron and hole pairs could not be generated by the light (λ > 580 nm). The averaged wavelength (415 nm) was used in the calculating process of the AQY values. Similar processes were used for the calculations of AQYs of SnS_2-x series samples (Table S4).

Supporting Figures

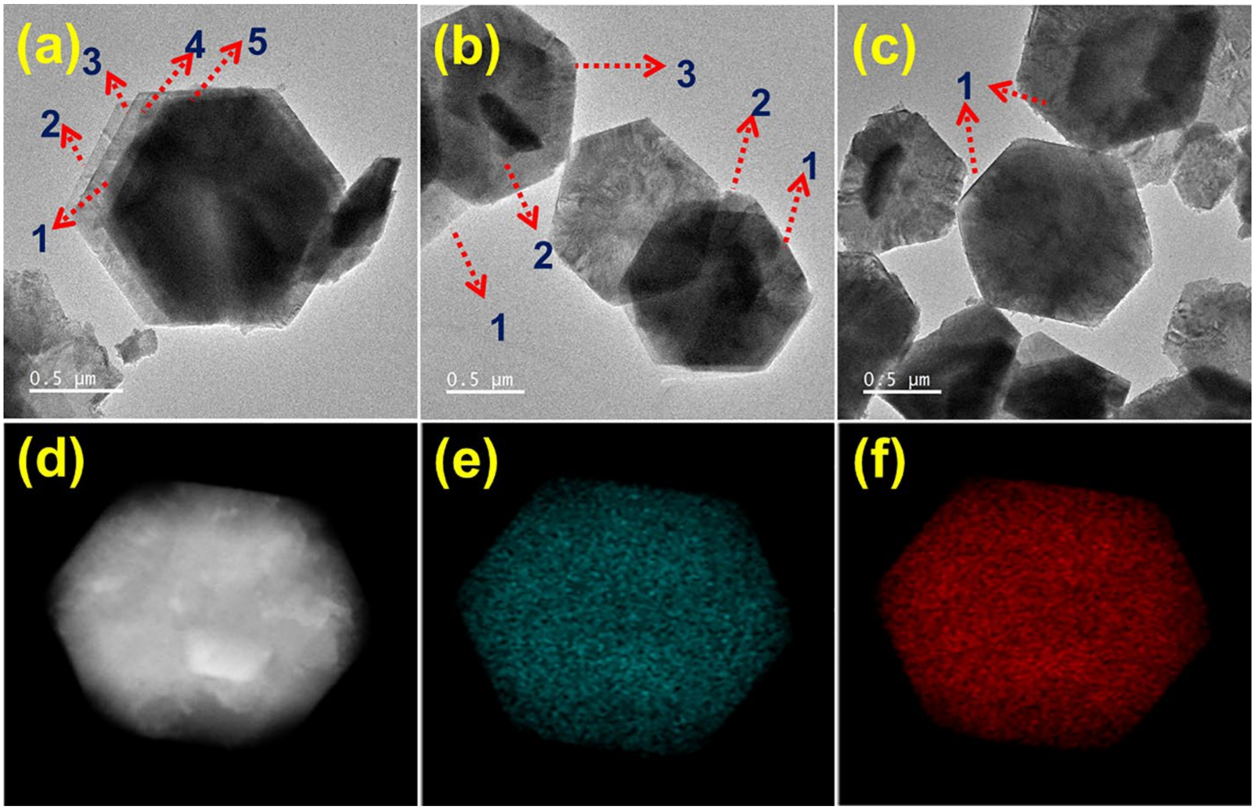

Fig. S1 TEM images of (a) SnS_2-160, (b) SnS_2-180, and (c) SnS_2-200. EDX element mappings of SnS_2-200 for (d) HAADF, (e) Sn and (f) S elements.

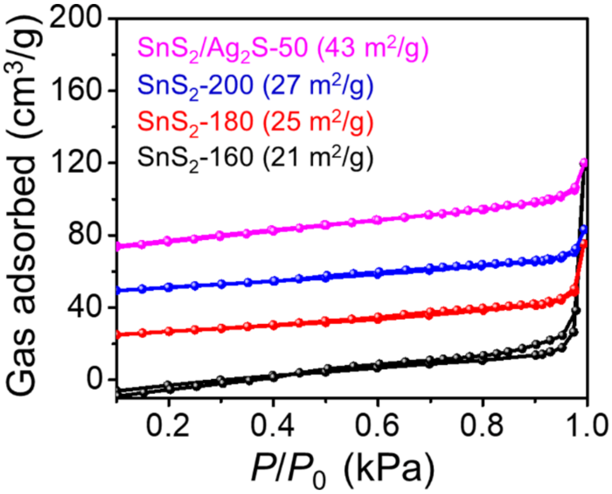

Fig. S2 Liquid N_2 adsorption-desorption isotherms of the SnS_2-x and the SnS_2/Ag_2S-50.

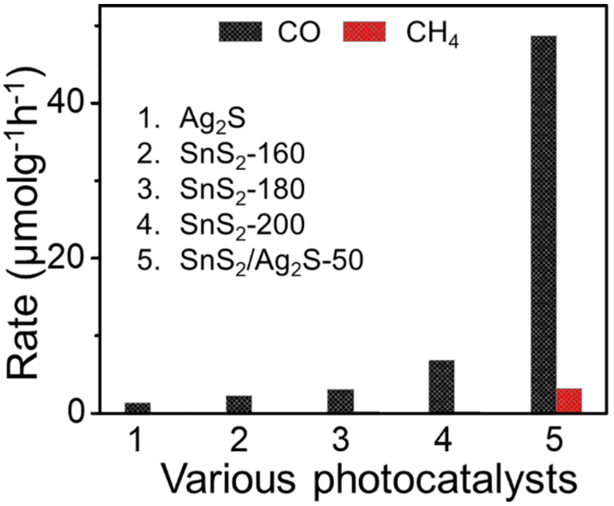

Fig. S3 Photocatalytic activity of pure Ag_2S and SnS_2-*x* with different reaction temperature in comparison to SnS_2/Ag_2S-50 composite.

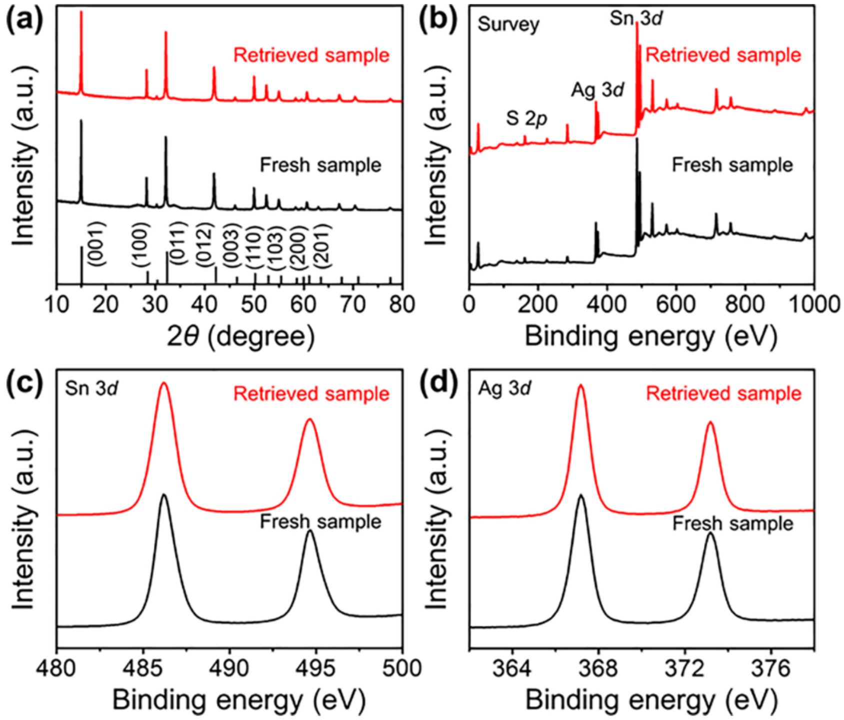

Fig. S4 (a) XRD and (b-d) XPS spectra of the photocatalyst SnS_2/Ag_2S-50 after four consecutive photocatalytic mesurements.

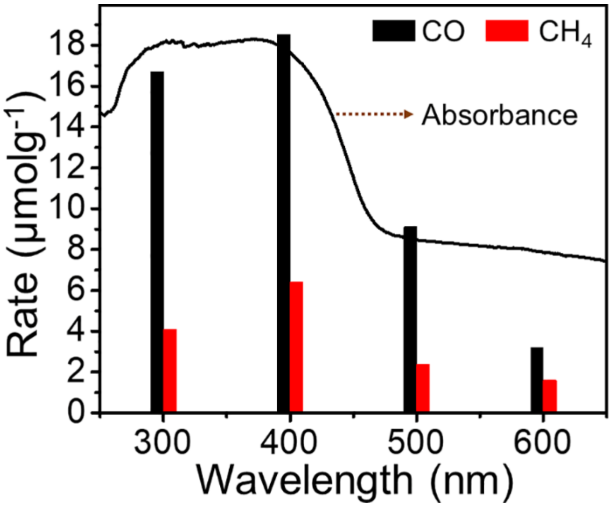

Fig. S5 Wavelength dependent photocatalytic activity of SnS_2/Ag_2S-50 composite for 10 h of photocatalytic reactions.

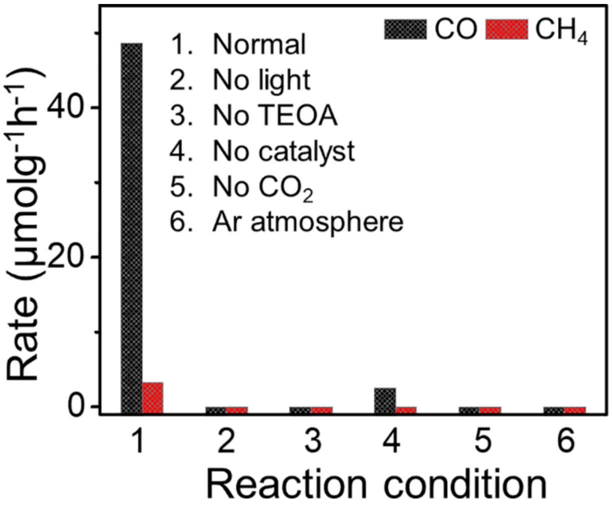

Fig. S6 The comparative assessments for the photoactivity of SnS_2/Ag_2S-50 under different experimental conditions.

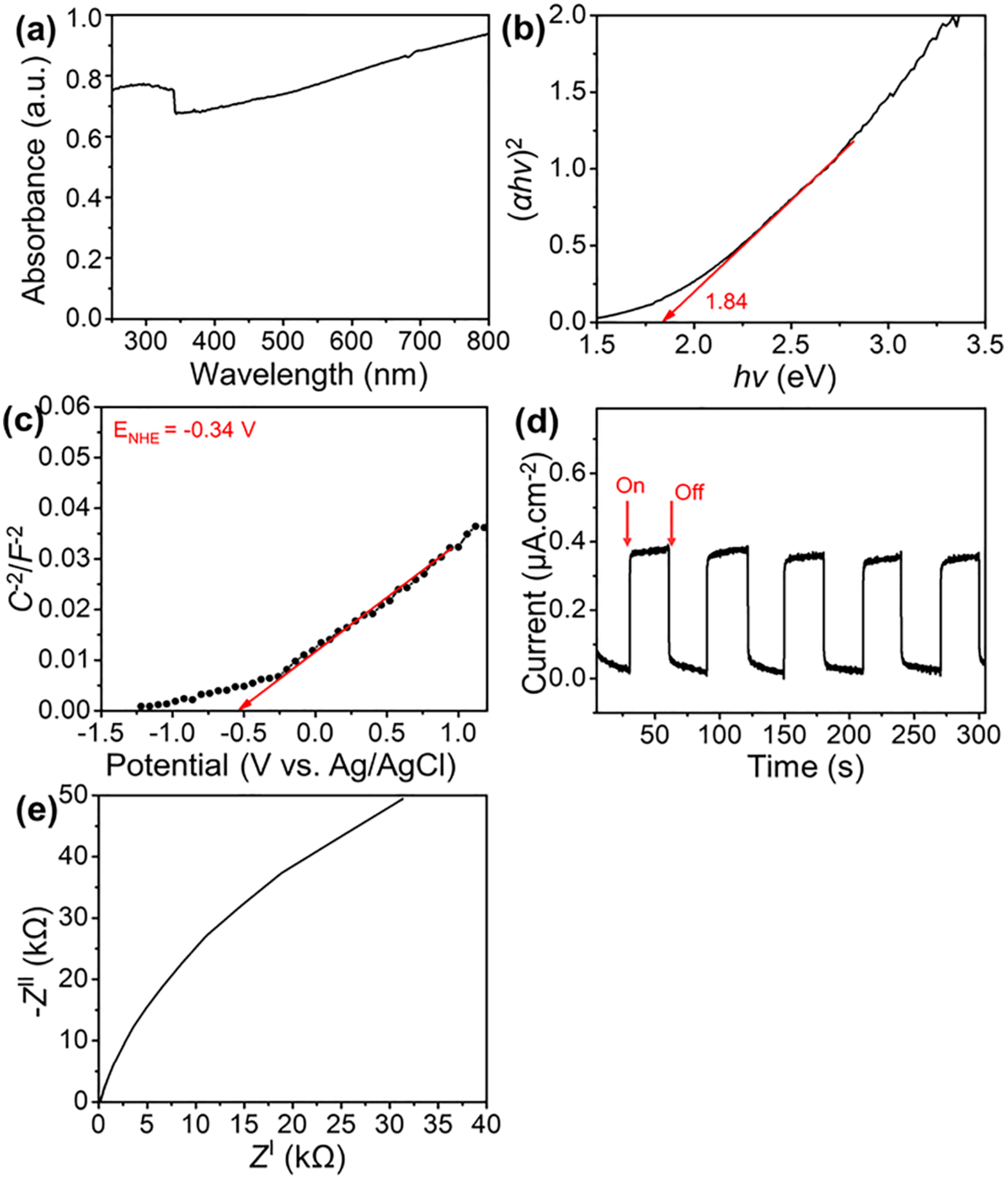

Fig. S7 Photophysical and photoelectrochemical properties of synthesized Ag_2S: (a) DRS absorption spectrum, (b) calculated Tauc plot from DRS spectrum, (c) Mott-Schottky curve, (d) photocurrent responses, and (e) electrochemical impedance spectrum.

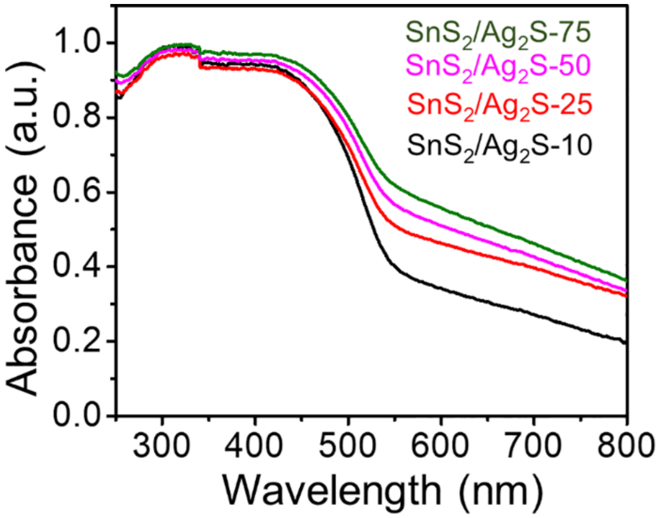

Fig. S8 DRS spectra of SnS_2/Ag_2S composites with different Ag_2S contents.

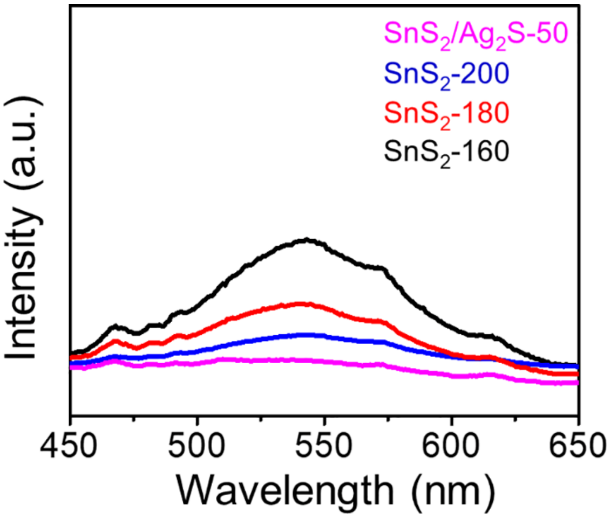

Fig. S9 Photoluminescence spectra of the SnS_2-*x* and the SnS_2/Ag_2S-50.

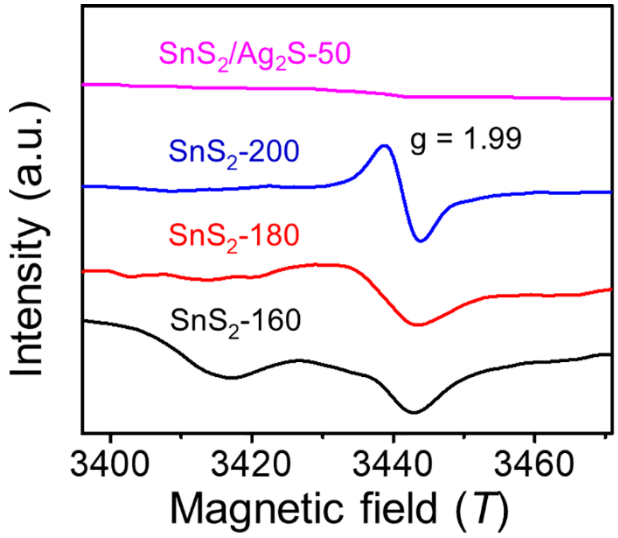

Fig. S10 EPR spectra for SnS_2-*x* samples and the SnS_2/Ag_2S-50.

Supporting Tables

Table S1 EDX elemental compositions of SnS_2 obtained from 200 ℃ and SnS_2/Ag_2S-50 nanocomposites by EDS data.

Sample	Sn (wt%)	S (wt%)	Ag (wt%)	Ag_2S (wt%)	SnS_2 (wt%)
SnS_2-200	60.19	39.81	0	0	100
SnS_2/Ag_2S-50	56.13	34.37	9.50	33.6	66.4

Table S2 Fluorescence decay data of the SnS_2-*x* and the SnS_2/Ag_2S-50 composites excited and detected by 373 and 543 nm light, respectively.[a]

Sample	SnS_2-160	SnS_2-180	SnS_2-200	SnS_2/Ag_2S-50
$\tau_{1\ /\ \mathrm{ns}}$	1.61	2.10	2.36	1.60
$\tau_{2\ /\ \mathrm{ns}}$	0.18	0.19	0.20	0.18
$\tau_{\mathrm{ave}\ /\ \mathrm{ns}}$	0.21	0.24	0.25	0.22

[a] τ_1 and τ_2 are the fitted fluorescence lifetime and τ_{ave} is the average fluorescence lifetime of the corresponding system.

Table S3 Calculated TCEN for the SnS_2-*x* and the SnS_2/Ag_2S-50 nanocomposites.

Sample	SnS_2-160	SnS_2-180	SnS_2-200	SnS_2/Ag_2S-50
TCEN (μmol g^{-1} h^{-1})	5	8.5	14	123

Table S4 Calculated AQY for the SnS_2-*x* and the SnS_2/Ag_2S-50 nanocomposites.

sample	SnS_2-160	SnS_2-180	SnS_2-200	SnS_2/Ag_2S-50
AQY (%)	0.008	0.014	0.023	0.42